Regular Article

PHYSICAL CHEMISTRY RESEARCH
Published by the
Iranian Chemical Society
www.physchemres.org
info@physchemres.org

Phys. Chem. Res., Vol. 7, No. 4, 799-812, December 2019
DOI: 10.22036/pcr.2019.199338.1669

Antimicrobial Investigation of CuO and ZnO Nanoparticles Prepared by a Rapid Combustion Method

R. Shashanka[a,*], Y. Kamacı[a], R. Taş[b], Y. Ceylan[c], A. Savaş Bülbül[d], O. Uzun[e,f] and A. Cahit Karaoglanli[a]

[a]*Bartın University, Department of Metallurgical and Materials Engineering, Bartın, Turkey*
[b]*Bartın University, Department of Biotechnology, Bartın, Turkey*
[c]*Bartın University, Department of Molecular Biology and Genetics, Bartın, Turkey*
[d]*Kahramanmaraş Sütçü İmam University, Department of Biology, Kahramanmaraş, Turkey*
[e]*Rectorate of Bartın University, Bartın, Turkey*
[f]*Ankara University, Department of Physics, Ankara, Turkey*
(Received 26 August 2019, Accepted 26 September 2019)

In recent years, fabrication of metal oxide nanoparticles is intensively gaining the interest of various chemists as well as biochemist due to their applications in different fields. Among all the transition metal oxides, CuO and ZnO are the important metal oxide nanoparticles exhibiting tremendous properties and a wide range of applications. Both CuO and ZnO nanoparticles were prepared by combustion method effectively with very less time. The combustion of copper(II) nitrate and urea at stoichiometric ratio results in CuO nanoparticles. Similarly, combustion of zinc(II) nitrate and urea at stoichiometric ratio results in ZnO nanoparticles. Both CuO and ZnO nanoparticles were characterized by X-ray diffraction to study the different phases present in them. The microstructure and composition of the prepared metal oxide nanoparticles were studied using scanning electron microscopy (SEM) and energy dispersive spectroscopy attached to SEM, respectively. The optical studies were carried out using UV-Vis spectrophotometer. Particle size analyser was used to determine the mean average particle size of the prepared metal oxide nanoparticles. The CuO and ZnO NPs were applied to gram-negative and gram-positive bacteria using minimum inhibition concentration (MIC) assay which demonstrated an essential antibacterial effect.

Keywords: Combustion method, Metal oxide nanoparticles, Bandgap energy, Minimum inhibition concentration, Antimicrobial activity

INTRODUCTION

The science and technology of nanomaterial research is one of the most attractive and promising fields for the utmost development in this modern era [1,2]. Generally, terms like nanoparticles, nanocrystals, nanofibers, nanotubes and nanocomposites are used in the field of nanoscience, and technology. Nanostructured materials exhibit different properties when compared to other materials in their bulk form [3-6]. In recent years, synthesis of metal oxide nanoparticles is advancing with great momentum due to its ability to produce materials in nanoscale and their applications in various fields. One of the main advantages of preparing metal oxide nanoparticles is their extremely small size and high surface ratio. Due to their extremely refined size; the metal nanoparticles have unique physical and chemical properties compared to nano metals. Some of the important metal oxide nanoparticles are CuO, ZnO, TiO_2, Fe_2O_3, Al_2O_3, MgO, AgO, CeO_2, ZrO_2, *etc*. [7]. Among all, CuO and ZnO nanoparticles have a wide range of properties and applications. Therefore, the authors decided to prepare both CuO and ZnO nanoparticles and studied their properties.

Copper oxide (CuO) nanoparticles are one of the very

*Corresponding author. E-mail: shashankaic@gmail.com

useful metal oxides and appear to be brownish-black powder. The properties like high electrical conductivity, toughness, excellent ductility, high hardness and luminescent efficiency of semiconductors have made CuO nanoparticles as one of the valuable metal oxides [8]. Due to the wide variety of properties, CuO nanoparticles can be used as burning rate catalyst in rocket propellant, catalyst, superconducting materials, thermoelectric materials, sensing materials, ceramic resistors, magnetic storage media, gas sensors, photoconductive and photothermal materials, solar energy transformation, high-tech superconductors, and semiconductors. The CuO nanoparticles are semiconducting in nature in the nano range and behave differently with the increase in the sizes. Semiconducting nature of CuO nanoparticles is very useful in fabricating electronic and optoelectronic devices like electrochemical cell, magnetic storage devices, gas sensors, nano fluid, field emitters and catalysts [9].

Another important class of metal oxide nanoparticles are zinc oxide (ZnO); they are available as white powders and dispersions. The general properties of ZnO nanoparticles include antibacterial, anti-corrosive, antifungal and UV filtering properties. Zinc oxide is one of the metal oxides having a wide range of applications. ZnO nanoparticles are mainly used in the manufacturing of rubber, cigarettes (used as a filter), beauty products (popularly known calamine lotion), ointment to treat skin diseases, as an additive in food products such as breakfast cereals, and as an additive in manufacturing of concrete and paints [10]. The ZnO nanoparticles exhibit a wide bandgap, and doping can be done in oxygen vacancies or zinc interstitials is n-type [11]. The ZnO nanoparticles have unique semiconductor properties, such as good transparency, high electron mobility, wide bandgap, and strong room-temperature luminescence. These unique properties of ZnO nanoparticles are used in transparent electrodes in liquid crystal displays, energy-saving or heat-protecting windows and light-emitting diodes [12].

The properties of all the metal or metal oxide nanoparticles mainly depend upon size, morphology, phases and specific surface area. Some aspects strongly depend on preparation methods. Nanomaterials can be prepared by different methods like sol-gel method [13], deposition method [14], chemical methods [15], mechanical alloying [16-20], physical methods, and various biological methods [2]. However, among all, combustion synthesis is an effective method for the easy synthesis of nanostructured materials. It has been used in the production of various metals and metal oxide nano powders for a variety of advanced applications. Combustion synthesis is also called as self-propagating high-temperature synthesis (SHS) which is an effective, low-cost method for production of various industrially useful materials [21]. A significant number of important ground-breaking studies have been reported in this field, especially for the development of new grades of catalysts and sensors with improved surface properties compared to the studies performed on the other traditional methods.

H. Sadabadi *et al.* [22] prepared monoclinic phase copper(II) oxide nanoparticles by combustion methods using an oxidiser copper nitrate and a fuel glycine. B. S. Anandakumar *et al.* [23] prepared black coloured powder of CuO nanoparticles by mixing copper nitrate trihydrate (an oxidizer) and malic acid (a fuel) at a temperature of 450 °C. They reported the use of prepared CuO nanoparticles as a potential catalyst for the rapid synthesis of aromatic nitriles from araldehydes. O. H. Abd-Elkader *et al.* [24] synthesised CuO nanoparticles using glycine assisted combustion method. In this method, they mixed calculated proportions of copper nitrate with different amounts of glycine in a porcelain crucible placed on a hot plate at 350 °C for 5 min to produce brown fluffy CuO nanoparticles. K. Jhansi *et al.* [25] used cupric nitrate and citric acid to prepare CuO nanoparticles by combustion method and reported the possible use of prepared CuO nanoparticles as a humidity sensor.

N. N. H. Shah *et al.* [26] prepared ZnO nanoparticles using a cost-effective modified combustion method by mixing zinc nitrate hexahydrate and palm oil derived C8 fatty alcohol in different ratios. They reported that the prepared nanoparticles exhibit hexagonal wurtzite structure and the crystallite size range was between 28-40 nm. M. Kooti *et al.* [27] reported an efficient and cost-effective combustion method for the synthesis of ZnO nanoparticles using glycine and zinc nitrate as precursors. V. Kumar *et al.* [28] and A. C. Lucilha *et al.* [29] used combustion method to prepare ZnO nanoparticles by mixing an appropriate proportion of zinc nitrate and urea on a hot plate until the

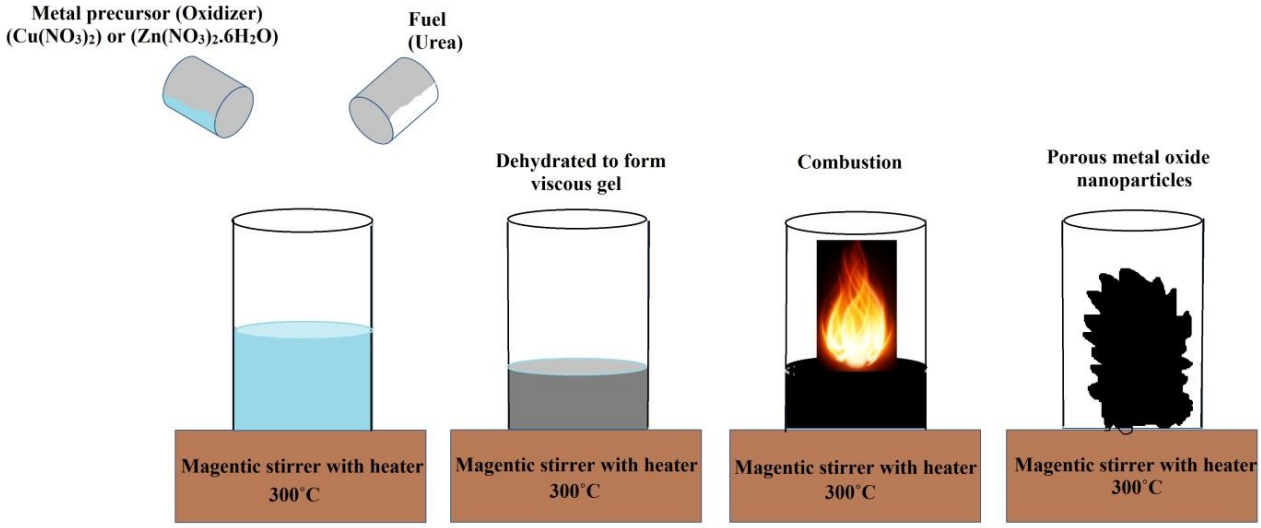

Fig. 1. Graphical representation of preparation of the metal oxide nanoparticles.

solution underwent strong combustion. They studied the magnetic properties and photocatalytic properties, respectively. D. Syamala Bai *et al.* [30] synthesized ZnO nanoparticles using low-temperature solution combustion method and investigated semiconducting properties at a temperature range of 320-385K.

Research carried out in the last few years across the world has proved the ability of combustion synthesis to improve the various properties of materials, energy-saving, and environmental protection (eco-friendly). It is not an easy task to produce nanomaterials by conventional methods [21,31-37]. Very little literature is available on the preparation of CuO and ZnO nanoparticles by combustion method. Keeping all the advantages of combustion synthesis in mind, here, we report the synthesis of CuO and ZnO nanoparticles by combustion method.

EXPERIMENTAL

The experimental procedure to prepare CuO and ZnO metal oxide nanomaterials is as follows.

Preparation of CuO Nanoparticles

Chemicals required. (i) Copper(II) nitrate ($Cu(NO_3)_2$) (ii) Glycine or urea or sucrose or DL-Malic acid.

Method. Dissolve 5 g of copper(II) nitrate and 5 g of urea in 20 ml distilled water. Stir the solution for homogeneity and keep the reaction solution in a silica crucible. Heat the reaction mixture on a magnetic stirrer at 300 °C. Initially, the viscous gel undergoes dehydration and combustion starts which results in a porous nanocrystalline black-coloured product. This black coloured powder is CuO nanoparticles.

Preparation of ZnO Nanoparticles

Chemicals required. (i) Zinc(II) nitrate ($Zn(NO_3)_2.6H_2O$)
(ii) Urea or sucrose or DL-Malic acid

Method. (a) Dissolve 3 g of zinc(II) nitrate and 1.5 g of urea in 20 ml distilled water. Stir the solution for homogeneity and keep the reaction solution in a silica crucible. Heat the reaction mixture on a magnetic stirrer at 300 °C [38]. Initially, the viscous gel undergoes dehydration and start combustion and results in brown transparent viscous gel and later results in white coloured ZnO nanoparticles.

The graphical representation of the preparation of metal oxide nanoparticles is shown in Fig. 1.

Phase analysis of CuO and ZnO nanoparticles was carried out using XRD (RIGAKU SmartLab) in the 2θ range at 30-70° using Cu $Ka_{\alpha 1}$ radiation (λ = 1.54056 Å). The morphology of the metal oxide nanoparticles was studied using scanning electron microscopy (SEM)

(TESCAN-MAIA3 XMU). Quantification of the elements present in the prepared nanoparticles was studied by energy dispersive spectroscopy (EDS) attached to SEM. Optical properties were studied using UV-Vis spectroscopy (Shimadzu-UV 3600 Plus); where bandgap was calculated. Particle size analyser (Malvern- Mastersizer 3000) was used to determine the average mean particle size of the prepared metal oxide nanoparticles.

All the research work starting from the preparation of the CuO and ZnO nanoparticles and their characterizations were performed at Bartin University, Turkey. Further antimicrobial activity of prepared metal oxide nanoparticles was studied.

RESULTS AND DISCUSSION

Figure 2 shows the XRD diffraction pattern of CuO nanoparticles prepared by combustion method. From Fig. 2, the sharp peaks at 2θ of 35.59°, and 38.79° correspond to (002) and (111) planes, respectively, confirming the formation of single-phase CuO with monoclinic structure. The diffraction peaks are broadened due to the nanostructure of the prepared CuO nanoparticles. The average crystallite size of CuO nanoparticles is calculated by Scherrer's formula as follows [39],

$$D = \frac{K\lambda}{\beta \cos\theta} \quad (1)$$

where D = Average crystallite size, K = A constant equal to 0.94, λ = The wavelength of X-ray radiation (0.154 nm), β = Full-width half maximum of the peak (in radians), and 2θ = Bragg's angle (degree).

By using the Eq. (1), we calculated the crystallite size for the peaks (002) and (111), and the values found to be ~14 nm and ~12 nm, respectively.

Similarly, Fig. 3 depicts the XRD pattern of ZnO nanoparticles prepared by combustion method. The diffraction peaks at 2θ of 31.73°, 34.41° and 36.23° correspond to the diffraction peaks (100), (002) and (101), respectively, confirming the formation of hexagonal wurtzite structure of ZnO. The peaks are broadened and no peak could be attributed to impurity, confirming that the synthesized ZnO nanoparticles are highly pure and nano-crystalline. The average crystallite size of CuO nanoparticles is calculated to the diffraction peaks (100), (002) and (101) by Scherrer's formula [39] and the values found to be ~ 15 nm, ~ 12 nm and ~ 13 nm, respectively.

Microstructural analysis of the prepared metal oxide nanoparticles is performed using SEM. Metal oxide nanoparticles prepared from combustion method result in loosely bound and porous structure due to the release of an enormous amount of gases [9]. Figure 4 represents the SEM image of the low magnified general porous structure of the prepared ZnO nanoparticles. From the figure, we can observe how the small spherical particles linked one by one to form a giant porous structure.

Even though combustion reactions produce homogenous material of small and uniform nanoparticles, sometimes, due to the high temperature during combustion reaction, they result in the non-uniform and wide size range of particles because of agglomeration chances. Figure 5a depicts the SEM image of CuO nanoparticles prepared by the combustion method. SEM image shows that CuO nanoparticles appear spongy where the nanoparticles are linked together to form agglomerates of different sizes and shapes. Ultimately, we have prepared CuO nanoparticles to exhibit both spherical and rod shapes as shown in the figure. The size of spherical CuO is found to be 60-100 nm, whereas, the sizes of CuO nanorods are found to be 500 nm width and 3 μm length, respectively.

The EDS analysis was performed to study the composition of elements present in the prepared metal oxide nanoparticles. Figure 5b shows the energy dispersive spectroscopy analysis of CuO nanoparticles. Theoretically, the atomic percentage of metals (Cu) and oxygen should be 50% each. Experimentally, the atomic percentage of copper and oxygen are found to be 50% and 50%, respectively.

Similarly, Fig. 6a shows the SEM image of ZnO nanoparticles prepared by combustion method. SEM image shows that ZnO nanoparticles appears spongy and are spherical in nature linked together to form a big porous structure. Prepared ZnO nanoparticles exhibit very fine size and spherical shape as shown in the figure. The size of spherical ZnO nanoparticles is found to be between 15-19 nm according to the SEM image.

Figure 6b represents the EDS image of ZnO nanoparticles, and the atomic percentage of zinc and oxygen

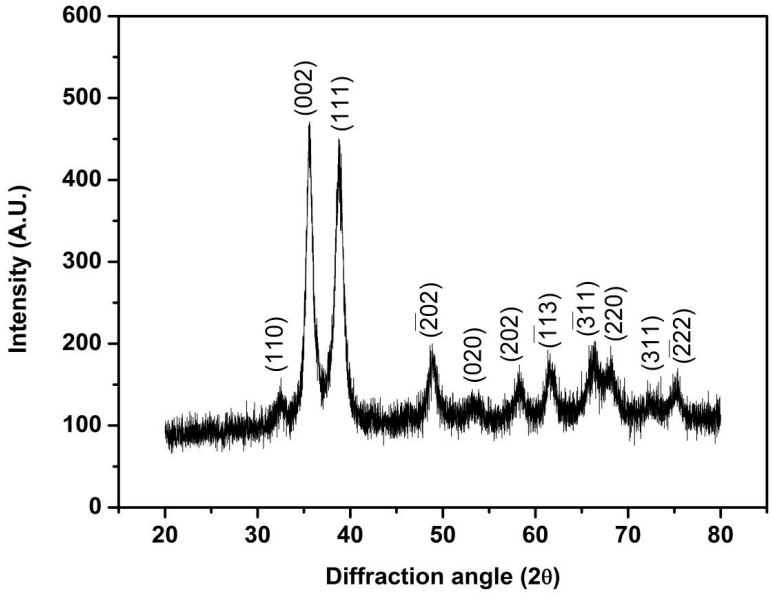

Fig. 2. XRD diffraction pattern of CuO nanoparticles prepared by combustion method.

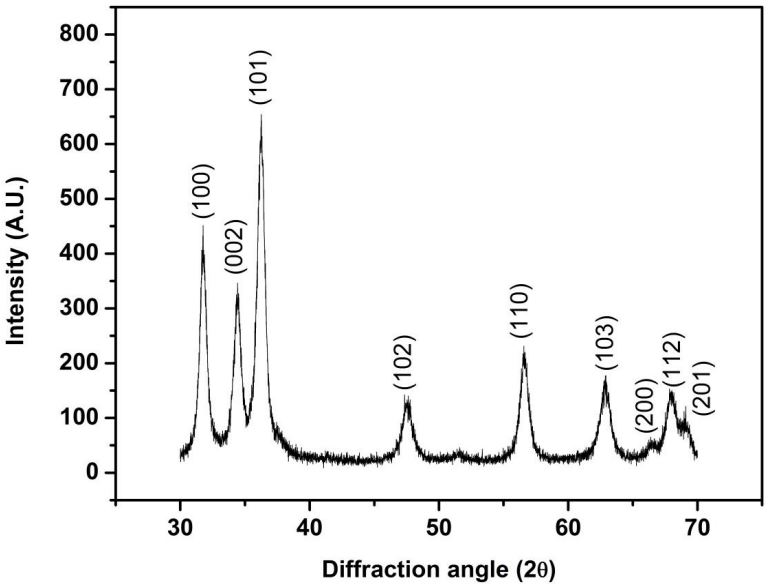

Fig. 3. XRD pattern of ZnO nanoparticles prepared by combustion method.

are theoretically and experimentally found the same (50% of Zn and 50% of Oxygen). As shown by the EDS data of both metal oxide nanoparticles, they are stoichiometric and agree with the theoretical values. Aparna *et al.* reported that if the particle size is less than 20 nm then they exhibit more strain, and if the size is greater than 20 nm then particles show less strain [9]. As we see from the particle size from SEM images of both CuO and ZnO nanoparticles, it clearly confirms that the ZnO nanoparticles show maximum strain than the CuO nanoparticles.

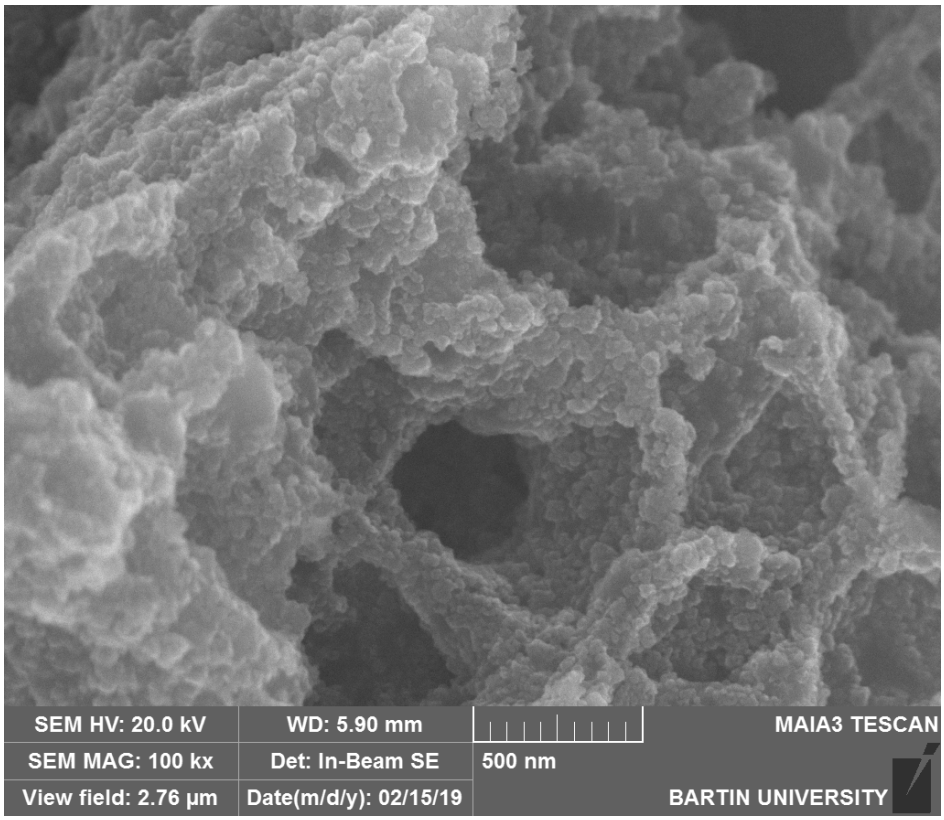

Fig. 4. SEM image of the low magnified general porous structure of ZnO nanoparticles prepared by combustion method.

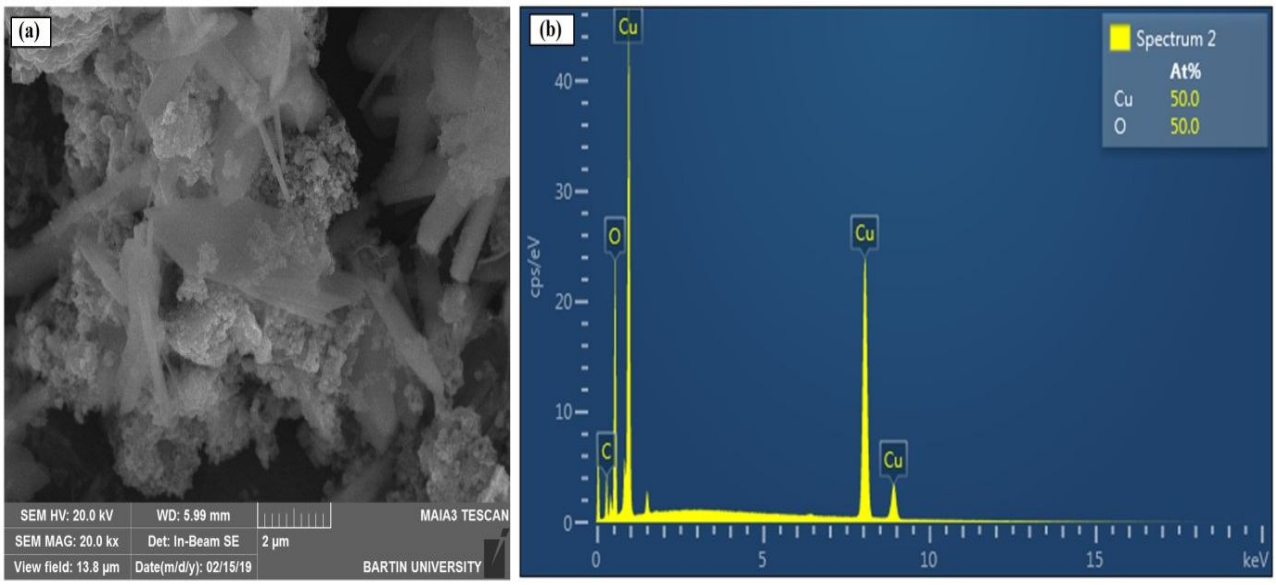

Fig. 5. (a) SEM image, and (b) EDS of CuO nanoparticles prepared by combustion method

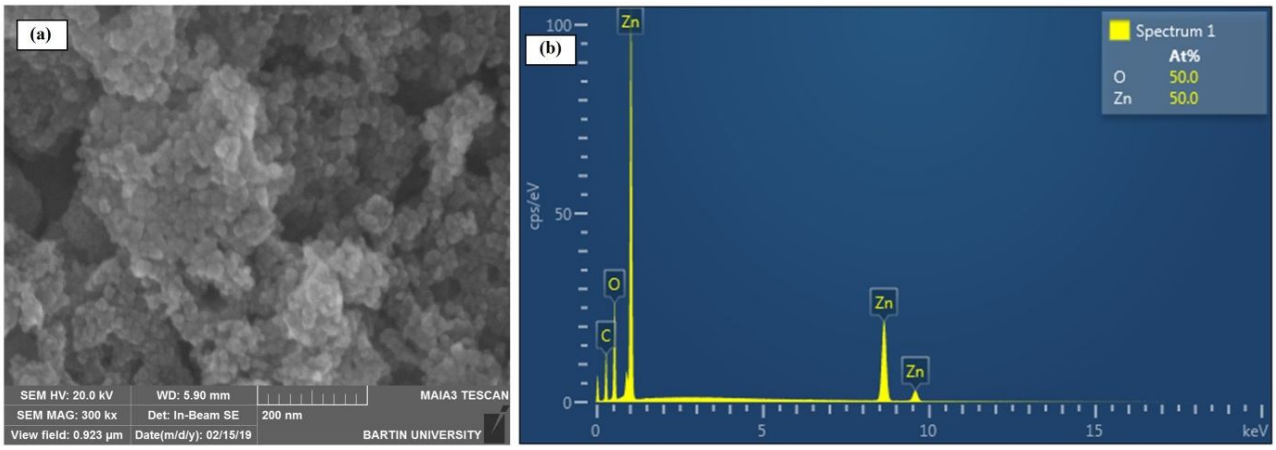

Fig. 6. (a) SEM image, and (b) EDS of ZnO nanoparticles prepared by combustion method.

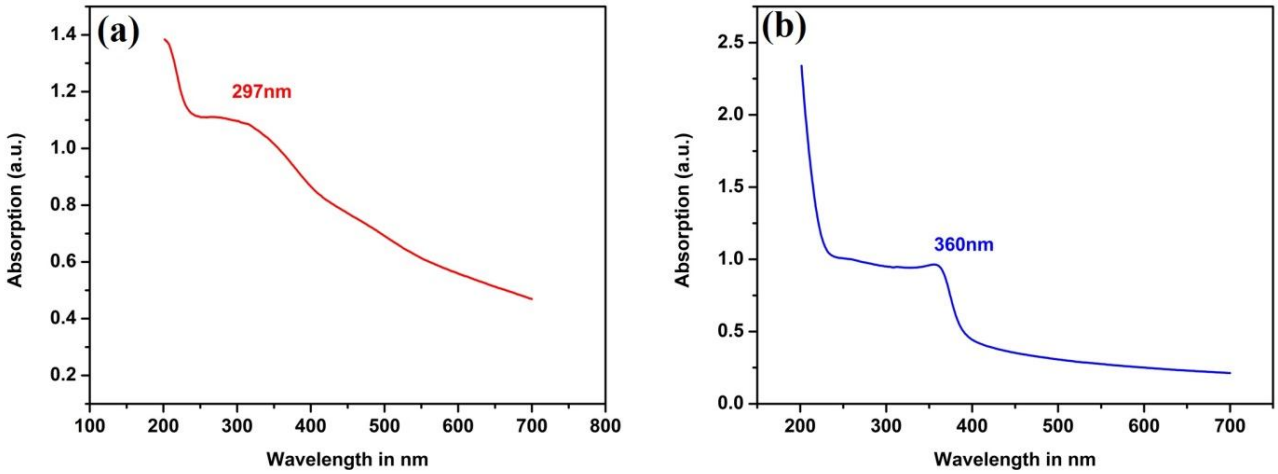

Fig. 7. UV-Vis spectra of (a) CuO, and (b) ZnO nanoparticles prepared by combustion method.

The UV-Vis spectroscopy was used to study the optical properties of the prepared CuO and ZnO nanoparticles. Figure 7a depicts the UV-visible spectra of CuO nanoparticles prepared by combustion method. Due to the presence of absorption edge, the type of transition and bandgap value can be determined [40,41]. Figure 7a shows a broad absorption peak at 297 nm which confirms the bandgap is due to the intrinsic transition of CuO [40]. The absorption spectra of CuO nanoparticles show a slightly weak fundamental absorption edge approximately in the range of 219 nm due to the direct transition of electrons [40]. The bandgap energy (E) of prepared CuO nanoparticles were calculated using the following equation [42],

$$E = \frac{h \times C}{\lambda} \quad (2)$$

where E = Bandgap energy

h = Planks constant = 6.626×10^{-34} Joules s

C = Speed of light = 3.0×10^{8} meter/s

λ = Cut off wavelength = 297×10^{-9} meters

*Conversion 1eV = 1.6×10^{-19} Joules

The calculated band gap energy value was found to be 4.18 eV which was higher than the bulk bandgap value of 3.5 eV [40]. This enhanced band gap energy value may due to the presence of intra-gap states and quantum confinement effect [40]. The CuO exhibits the bandgap energy more than 4 eV will behave as a photocatalyst.

Figure 7b depicts the UV-Vis spectra of ZnO nanoparticles prepared by combustion method. The UV-Vis spectrum shows a characteristic absorption peak of ZnO at a wavelength of 360 nm indicating that the bandgap is due to the intrinsic transition of CuO. This intrinsic bandgap absorption of ZnO is due to the electron transitions from the valence band to the conduction band [43,44]. Absorption peak looks sharp because of the nano-sized ZnO particles, and that their particle size distribution is narrow and monodispersing [45,46] (as confirmed by the SEM image of ZnO nanoparticles; Fig. 5). The bandgap energy (E) of prepared ZnO nanoparticles were calculated using the Eq. (2). The calculated band gap energy value of ZnO nanoparticles was found to be 3.44 eV. The intense absorption of the ZnO nanoparticles in the UV region results in the medical application such as sunscreen protectors or as antiseptic ointments.

Particle size analyser was used to measure the particle size distribution of CuO and ZnO nanoparticles. A solution of CuO and ZnO was prepared separately with distilled water and agitated in an ultra-sonicator for few minutes to get an evenly dispersed solution. The instrument was set to zero by measuring the background correction using the solvent (water) only, and then the CuO and ZnO solutions were filled in the cell separately to measure the average particle size. Particle size distributions of CuO nanoparticles are shown in Fig. 8. As we see from the figure, the particle size distribution curve of CuO nanoparticles exhibit two strong peaks (peak 1 and peak 2). According to SEM image of CuO nanoparticles, they show both spherical and rod-shaped structure. Peak 1 curve is due to the fine spherical particles of CuO nanoparticles, whereas, peak 2 curve corresponds to rod-shaped particles; whose size is more. CuO nanoparticles in curve 1 were determined to be ~ 40 nm, whereas, CuO nanoparticles at curve 2 shows ~ 15 μm particle size. The particle size distribution curve of CuO nanoparticles shows a wide range of particle sizes ranging from nano to microns. This is due to the possible agglomeration of CuO nanoparticles due to the absence of capping agents during combustion synthesis.

Similarly, Fig. 9 depicts the particle size distributions of ZnO nanoparticles prepared by combustion method. SEM image of ZnO nanoparticles shows almost spherical and even-sized ZnO nanostructure. The particle size distribution curve shows three weak peaks (peak 1, peak 2 and peak 3) and these peaks are not as strong as CuO particle size distribution curve but confirm the presence of different sized ZnO nanoparticles.

Peak 1 shows the particle size of ~ 0.4 μm, peak 2 shows particle size of ~ 2 μm and peak 3 corresponds to the particle size of ~ 13 μm, respectively. The size distribution curve shows a wide range of particle sizes due to the absence of capping agents.

Figure 10 represents the mean average particle size of CuO and ZnO nanoparticles based on the percentage of cumulative passing. As we see from the graph, the mean average particle size of CuO nanoparticles was found to be 3.7 μm and that of ZnO nanoparticle was found to be 6.8 μm. The specific surface area of CuO and ZnO nanoparticles were found to be 52380 $m^2\ kg^{-1}$ and 2002 $m^2\ kg^{-1}$, respectively.

ANTIMICROBIAL ACTIVITY

Minimum Inhibition Concentration (MIC) and Minimum Bacteriocidal/Bacteriostatic Concentration (MBC)

The antibacterial properties of CuO and ZnO nanoparticles were tested against three gram-positive and gram-negative bacteria as *Enterobacter aerogenes, Klebsiella pneumoniae, Escherichia coli* CFAI, *Enterococcus faecalis, Staphylococcus epidermidis,* and *Bacillus subtilis*. The prepared copper oxide and zinc oxide nanoparticles were analysed to evaluate the minimum inhibition concentration (MIC) required for the growth of tested bacteria in this study. The CuO and ZnO solutions were prepared at 50 mg ml^{-1} concentration. Bacterial strains were inoculated to Luria Bertani broth and bacterial growths were standardized to 0.5 McFarland standard turbidity (1.5×10^8 CFU/ml). The LB broth and oxides at the same volume were added into the first well of 96 well plates and then two-fold dilutions of oxides were diluted from 50 mM

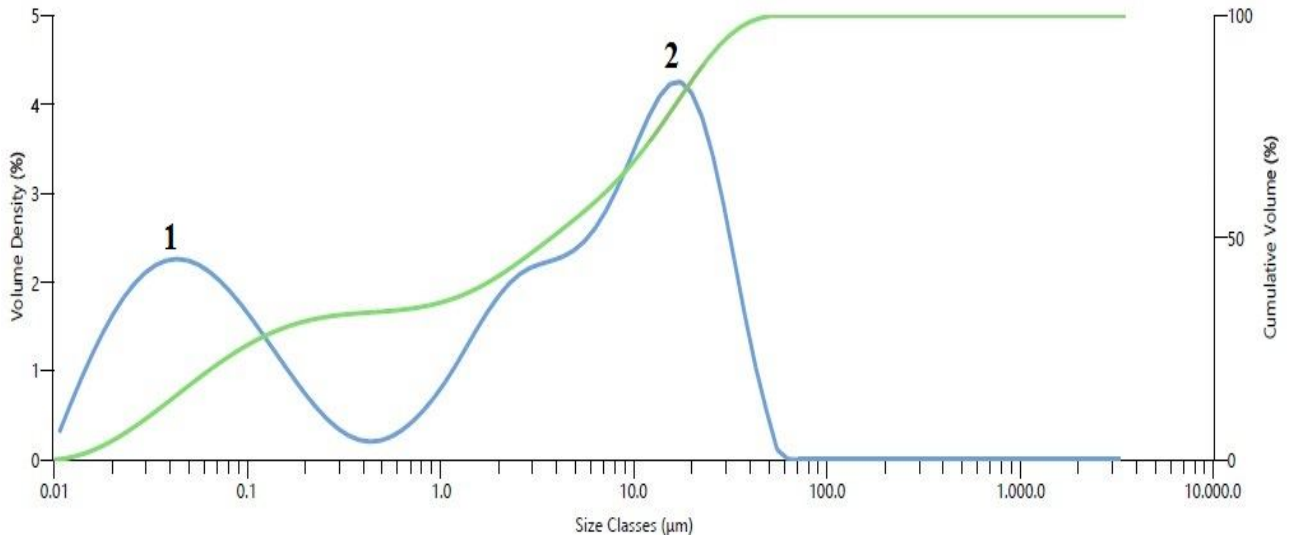

Fig. 8. Particle size distributions of CuO nanoparticles prepared by combustion method.

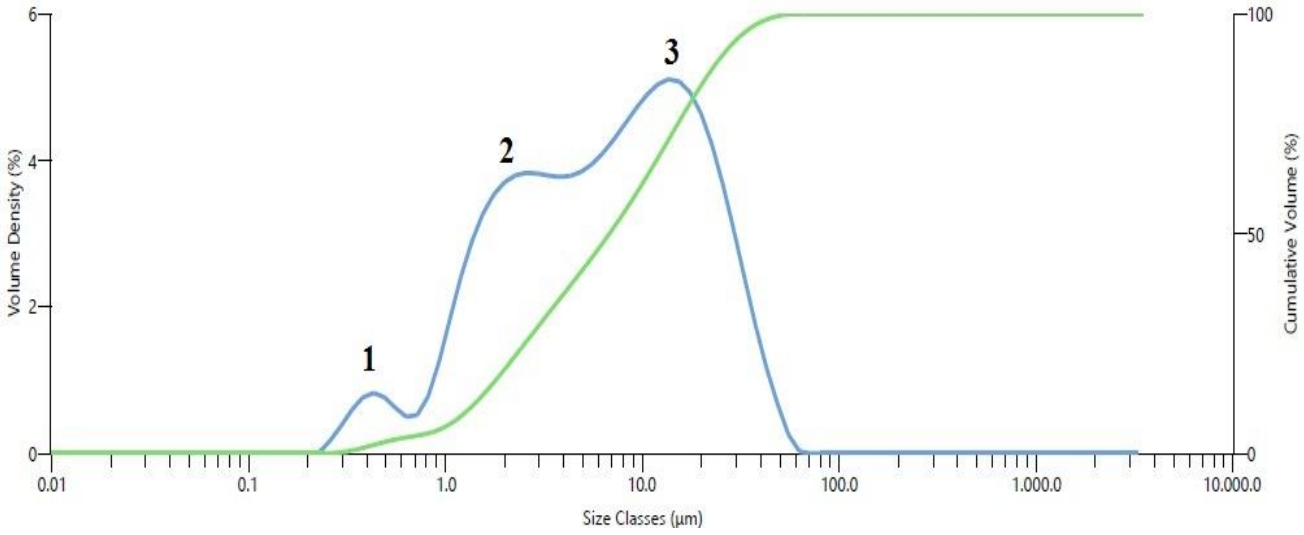

Fig. 9. Particle size distributions of ZnO nanoparticles prepared by combustion method.

to 1.5625 mM using 96-well microplate that was incubated at 37 °C for 24 h after inoculation. The MIC value was determined by UV-Vis spectrum at 600 nm. The next day, all wells in which no observable bacteria growth were tested in MIC assay were used for a further test called minimum bacteriostatic/bacteriocidal concentration (MBC). The wells for MBC were selected and streaked on LB-Agar plates and incubated at 37 °C for overnight.

As we mentioned earlier, the antibacterial properties of CuO and ZnO nanoparticles were investigated against six bacteria strains namely *Enterobacter aerogenes, Klebsiella pneumoniae, Escherichia coli* CFAI, *Enterococcus faecalis, Staphylococcus epidermidis,* and *Bacillus subtilis* using MIC and MBC assay. According to results, both the oxide nanoparticles showed antibacterial activity against tested bacteria (Table 1). Mostly, they demonstrated antibacterial

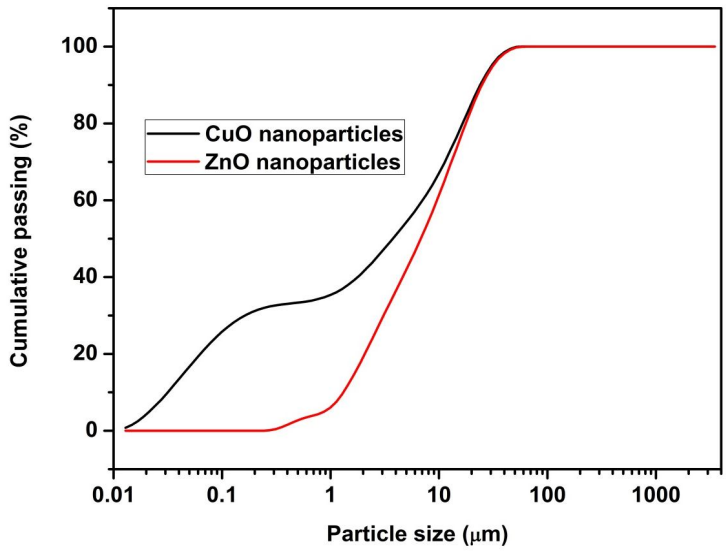

Fig. 10. The mean average particle sizes of CuO and ZnO nanoparticles on the basis of the percentage of cumulative passing.

Table 1. Antibacterial Effect of Zinc and Copper Oxides Concentration

Type of	50 mM		25 mM		12.5 mM		6.25 mM		3.125 mM		1.5625 mM	
bacteria	CuO	ZnO	CuO	ZnO	CuO	ZnO	CuO	ZnO	CuO	ZnO	CuO	ZnO
E.aerogenes	M	M										
K. pneumoniae	*	*	M	M								
E.coli CFAI		M										
E. faecalis	*	M	M									
S.epidermidis	M	M										
B. subtilis	M	M										

M: MIC value. *: MBC value.

effect at 50 and 25 mM concentrations only as shown in Fig. 11.

The antibacterial activity of copper oxide was studied in different studies. Jadhav *et al.* [47], Černik *et al.* [48], and Ananth *et al.* [49] examined the antibacterial properties of copper oxide nanoparticles against pathogen bacterias like gram (-) *E. coli* and gram (+) *S. aureus, Streptococcus iniae, Streptococcus parauberis* and *Vibrio anguillarum* at low concentration using MIC assay and reported the similar kind of results.

Similarly, the antibacterial activity of zinc oxide nanoparticles was studied by Xie *et al.* [50] and Sevinç

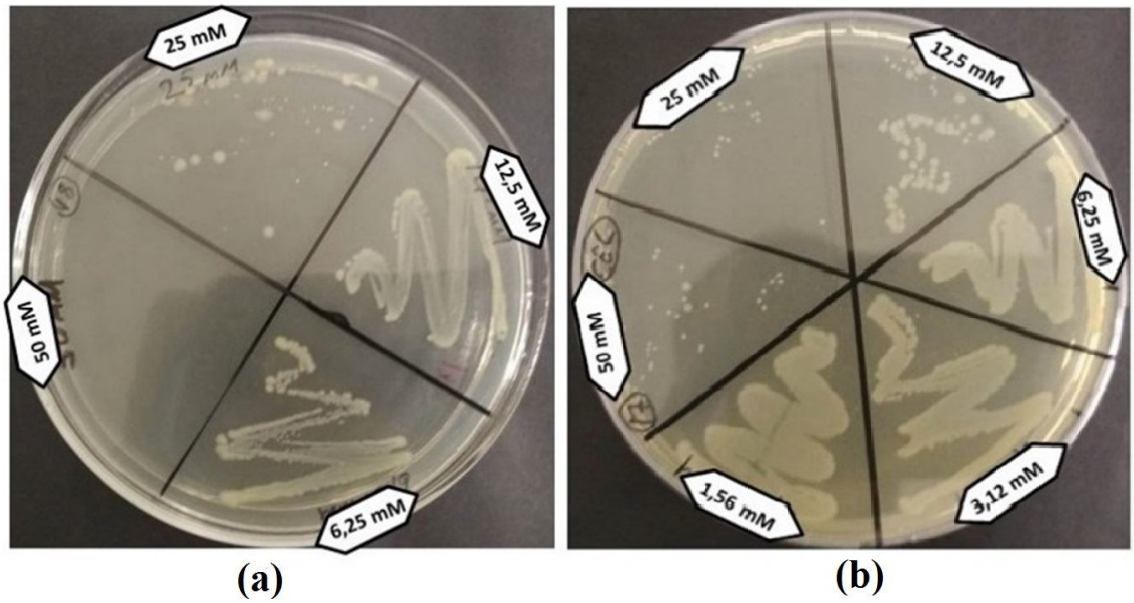

Fig. 11. The antibacterial effect of (a) CuO against E. faecalis, and (b) ZnO against *K. pneumoniae*.

et al. [51] at different concentrations of ZnO nanoparticles, and the similar kind of results were reported. In brief, both CuO and ZnO nanoparticles prepared by combustion method exhibit significant antibacterial effect and showed the lethal effect to some tested bacteria in this study. The results show that CuO and ZnO nanoparticles could be possibly conceived as an antibacterial agent to preserve food, agriculture and daily usage.

CONCLUSIONS

The combustion method of metal oxide nanoparticle synthesis is proved to be a very simple and robust technique. The CuO and ZnO nanoparticles were successfully prepared using urea as fuel and were characterized through XRD, SEM, UV-Vis spectroscopy, and particle size analyser. SEM images of CuO nanoparticles show both spherical and rod-shaped structure, whereas, ZnO nanoparticles show only spherical structure. The EDS data of both metal oxide nanoparticles confirm that they are stoichiometric and are in a good agreement with the theoretical values. UV-Vis spectroscopy of CuO nanoparticles depicts a broad absorption peak at 297 nm and the slightly enhanced band gap of 4.18 eV; this is due to the presence of intra-gap states and quantum confinement effect. Whereas, ZnO shows sharp absorption peak at a wavelength of 360 nm and the calculated band gap energy value was found to be 3.44 eV. Particle size analysis of CuO nanoparticles shows two strong peaks due to the different shapes of prepared CuO nanoparticles (Spherical and rod shape). The mean average particle size of CuO nanoparticles was found to be 3.7 μm and that of ZnO nanoparticle was found to be 6.8 μm. The particle size distribution curve of both metal oxide nanoparticles shows a wide range of particle sizes ranging from nano to microns due to the agglomeration of the prepared metal oxide nanoparticles. The antibacterial studies show that CuO and ZnO nanoparticles could be a potential candidate for an antibacterial material to preserve food, agriculture and daily usage.

REFERENCES

[1] Shashanka, R.; Chaira, D., Development of nano-structured duplex and ferritic stainless steel by pulverisette planetary milling followed by pressureless sintering. *Mater Charact.* **2015**, *99*, 220-229, DOI: 10.1016/j.matchar.2014.11.030.

[2] Shashanka, R.; Swamy, B. E. K.; Sathish, R.; Chaira, D., Synthesis of silver nanoparticles and their applications. *Anal. Bioanal. Electrochem.* **2013**, *5*, 455-466.

[3] Sathish, R.; Aruna, S.; Kumar, M.; Shashanka, R.; Jayadevappa, H., Preparation of NiO/ZnO hybrid nanoparticles for electrochemical sensing of dopamine and uric acid. *Chemical Sensors* **2012**, *2*, 1-7.

[4] Shashanka, R.; Chaira, D.; Swamy, B. E. K., Electrocatalytic response of duplex and yittria dispersed duplex stainless steel modified carbon paste electrode in detecting folic acid using cyclic voltammetry. *Int. J. Electrochem. Sci.* **2015**, *10*, 5586-5598.

[5] Shashanka, R.; Chaira, D., Phase transformation and microstructure study of nano-structured austenitic and ferritic stainless steel powders prepared by planetary milling. *Powder Technol.* **2014**, *259*, 125–136, DOI: 10.1016/j.powtec.2014.03.061.

[6] Shashanka, R.; Chaira, D., Optimization of milling parameters for the synthesis of nano-structured duplex and ferritic stainless steel powders by high energy planetary milling. *Powder Technol.* **2015**, *278*, 35-45, DOI: 10.1016/j.powtec.2014.03.061.

[7] Garcia, M. F.; Rodriguez, J. A., Metal Oxide Nanoparticles, Brookhaven National Laboratory, BNL-79479-2007-BC, 2007.

[8] AZoNano., Copper Oxide (CuO) Nanoparticles-Properties, Applications, 9th May, 2013.

[9] Aparna, Y.; Rao, K. V.; Subbarao, P. S., Preparation and characterization of CuO nanoparticles by novel sol-gel technique. *J. Nano- and Electronic Phys.* **2012**, *4*, 03005.

[10] AZoNano., Zinc Oxide (ZnO) Nanoparticles-Properties, Applications. 10th July, 2013.

[11] Özgür, Ü.; Alivov, Y.; Liu, C.; Teke, A.; Reshchikov, M. A.; Doğan, S.; Avrutin, V.; Cho, S. J.; Morkoç, H., A comprehensive review of ZnO materials and devices. *J. Appl. Phys.* **2005**, *98*, 041301, DOI: 10.1063/1.1992666.

[12] Wikipedia, Zinc Oxide, https://en.wikipedia.org/wiki/Zinc_oxide

[13] Eliseev, A. A.; Lukashin, A. V.; Vertegel, A. A.; Heifets, L. I.; Zhirov, A. I.; Tretyakov, Y. D., Complexes of Cu(II) with polyvinyl alcohol as precursors for the preparation of CuO/SiO_2 nanocomposites. *Mater. Res. Innov.* **2000**, *3*, 308-312.

[14] Malandrino, G.; Finocchiaro, S. T.; Nigro, R. L.; Bongiorno, C.; SpineIla, C.; Fragala, I. L., Free-standing copper(II) oxide nanotube arrays through an MOCVD template process. *Chem. Matter.* **2004**, *16*, 5559-5561, DOI: 10.1021/cm048685f.

[15] Gao, X. P.; Bao, J. L.; Pani, G. L.; Zhu, H. Y.; Huang, P. X.; Wu, F.; Song, D. Y., Preparation and electrochemical performance of polycrystalline and single crystalline CuO nanorods as anode materials for Li ion battery. *J. Phys. Chem. B* **2004**, *108*, 5547-5551, DOI: 10.1021/jp037075k.

[16] Shashanka, R.; Chaira, D.; Swamy, B. E. K., Electrochemical investigation of duplex stainless steel at carbon paste electrode and its application to the detection of dopamine, ascorbic and uric acid. *Int. J. Scientific & Engin. Res.* **2015**, *6*, 1863-1871.

[17] Nayak, A. K.; Shashanka, R.; Chaira, D., Effect of nanosize yittria and tungsten addition to duplex stainless steel during high energy planetary milling. *IOP Conf. Series: Materials Sci. Engin.* **2016**, *115*, 012008, DOI: 10.1088/1757-899X/115/1/012008.

[18] Shashanka, R.; Chaira, D.; Swamy, B. E. K., Fabrication of yttria dispersed duplex stainless steel electrode to determine dopamine, ascorbic and uric acid electrochemically by using cyclic voltammetry. *Int. J. Sci. Engin. Res.* **2016**, *7*, 1275-1285.

[19] Gupta, S.; Shashanka, R.; Chaira, D., Synthesis of nano-structured duplex and ferritic stainless steel powders by planetary milling: An experimental and simulation study. *IOP Conf. Series: Materials Sci. Engin.* **2015**, *75*, 012033, DOI: 10.1088/1757-899X/75/1/012033.

[20] Shashanka, R., Synthesis of nano-structured stainless steel powder by mechanical alloying-an overview. *Int. J. Sci. Engin. Res.* **2017**, *8*, 588-594.

[21] Aruna, S. T.; Mukasyan, A. S., Combustion synthesis and nanomaterials. *Curr. Opinion in Solid State and Mater. Sci.* **2008**, 12, 44-50, DOI: 10.1016/j.cossms.2008.12.002.

[22] Sadabadi, H.; Aftabtalab, A.; Zafarian, S.; Chakra.; Venkateswara, K. R.; Shaker, S., Influence of fuel and

condition in combustion synthesis on properties of copper(II) oxide nanoparticle. *Adv. Mater. Res.* **2014**, *829*, 152-156, DOI: 10.4028/www.scientific.net/AMR.829.152.

[23] Anandakumar, B. S.; Reddy, M. B.; Tharamani, C. N.; Pasha, M. A.; Chandrappa, G. T., Combustion-derived CuO nanoparticles: An effective and environmentally benign catalyst in the synthesis of aromatic nitriles from aromatic aldehydes. *Chinese J. Catal.* **2013**, *34*, 704-710, DOI: 10.1016/S1872-2067(11)60503-2.

[24] Omar, H. A.; Deraz, N. M., Synthesis and characterization of new copper based nanocomposite. *Int. J. Electrochem. Sci.* **2013**, *8*, 8614-8622.

[25] Jhansi, K.; Chandralingam, S.; Reddy, M. N.; Suvarna, P.; Ashok, C.; Rao, M. K., CuO nanoparticles synthesis and characterization for humidity sensor application. *J. Nanotech. Mater. Sci.* **2016**, *3*, 10-14, DOI: 10.15436/2377-1372.16.020.

[26] Shah, N. N. H.; Misran, H.; Razak, N. A. A.; Salim, M. A.; Othman, S. Z.; Manap, A., Modified combustion synthesis of ZnO nanoparticles using renewable fuel. *IOP Conf. Series: Earth and Environ. Sci.* **2013**, *16*, 012038.

[27] Kooti, M.; Sedeh, N. A., Microwave-assisted combustion synthesis of ZnO nanoparticles. *J. Chem.* **2013**, *2013*, 1-4. DOI: 10.1155/2013/562028.

[28] Kumar, V.; Kumar, S., Synthesis and characterization of ZnO nanoparticles using combustion method. *AIP Conf. Proc.* **2011**, *1393*, 331-332.

[29] Lucilha, A. C.; Afonso, R.; Silva, P. R. C.; Lepre, L. F.; Ando, R. A.; Dall'Antonia, L. H., ZnO Prepared by solution combustion synthesis: Characterization and application as photoanode. *J. Braz. Chem. Soc.* **2014**, *25*, DOI: 10.5935/0103-5053.20140085.

[30] Bai, D. S.; Kumar, V. R.; Suvarna, R. P., Synthesis and characterization of zinc oxide nanoparticles by solution combustion method: DC Conductivity studies. *Indian J. Adv. Chem. Sci.* **2017**, *5*, 137-*141*, DOI: 10.22607/IJACS.2017.503004.

[31] Manjunatha, J. G.; Deraman, M.; Basri, N. H., Electrocatalytic detection of dopamine and uric acid at poly (basic blue b) modified carbon nanotube paste electrode. *Asian J. Pharmaceut. Clin. Res.* **2015**, *8*, 48-53.

[32] Manjuntha, J. G.; Jayaprakash, G. K., Electrooxidation and determination of estriol using a surfactant modified nanotube paste electrode. *Eurasian J. Anal. Chem.* **2019**, *14*, 1-11, DOI: 10.29333/ejac/20190101.

[33] Manjuntha, J. G.; Deraman, M.; Basri, N. H.; Mohd Nor, N. S.; Talib, I. A.; Ataollahi, N., Sodium dodecyl sulfate modified carbon nanotubes paste electrode as a novel sensor for the simultaneous determination of dopamine, ascorbic acid, and uric acid. *Comptes Rendus Chimie* **2014**, *17*, 465-476, DOI: 10.1016/j.crci.2013.09.016.

[34] Manjuntha, J. G.; Kumara Swamy, B. E.; Mamatha, G. P.; Gilbert, O.; Srinivas, M. T.; Sherigara, B. S., Electrochemical studies of clozapine drug using carbon nanotube-SDS modified carbon paste electrode: A cyclic voltammetry study. *Der. Pharma. Chem.* **2011**, *3*, 236-249.

[35] Manjuntha, J. G.; Deraman, M.; Basri, N. H.; Talib, I. A., Fabrication of poly (Solid Red A) modified carbon nano tube paste electrode and its application for simultaneous determination of epinephrine, uric acid and ascorbic acid. *Arab. J. Chem.* **2018**, *11*, 149-158, DOI: 10.1016/j.arabjc.2014.10.009.

[36] Shashanka, R., Non-lubricated dry sliding wear behavior of spark plasma sintered nano-structured stainless steel. *J. Mater. Environ. Sci.* **2019**, *10*, 767-777.

[37] Shashanka, R., Effect of sintering temperature on the pitting corrosion of ball milled duplex stainless steel by using linear sweep voltammetry. *Anal. Bioanal. Electrochem.* **2018**, *10*, 349-361.

[38] Lian, X.; Li, Y.; Lv, T.; Zou, Y.; An, D.; Zhang, N., Preparation of ZnO nanoparticles by combustion method and their gas sensing properties. *Electron. Mater. Lett.* **2016**, *12*, 24-31, DOI: 10.1007/s13391-015-5293-5.

[39] Sharma, B. K.; Shah, D. V.; Roy, D. R., Green synthesis of CuO nanoparticles using azadirachta indica and its antibacterial activity for medicinal applications. *Mater. Res. Express.* **2018**, *5*, 095033, DOI: 10.1088/2053-1591/aad91d.

[40] Dhineshbabu, N. R.; Rajendran, V.; Nithyavathy, N.; Vetumperumal, R., Study of structural and optical

properties of cupric oxide nanoparticles. *Appl. Nanosci.* **2016**, *6*, 933-939, DOI 10.1007/s13204-015-0499-2.

[41] Essic, J.; Mather, R., Characterization of a bulk semiconductors band gap *via* near-absorption edge optical transmission experiment. *Am. J. Phys.* **1993**, *61*, 646-649, DOI: 10.1119/1.17173.

[42] Dharma, J.; Pisal, A., Application Note, UV/Vis/NIR Spectrometer, PerkinElmer, Inc. 940 Winter Street, Waltham, MA 02451, USA.

[43] Zak, A. K.; Razali, R.; Abd Majid, W. H.; Darroudi, M., 2011, Synthesis and characterization of a narrow size distribution of zinc oxide nanoparticles. *Int. J. Nanomed.* **2011**, *6*, 1399-1403, DOI: 10.2147/IJN.S19693.

[44] Zak, A. K.; Abrishami, M. E.; Abd Majid, W. H.; Yousefi, R.; Hosseini, S. M., Effects of annealing temperature on some structural and optical properties of ZnO nanoparticles prepared by a modified sol-gel combustion method. *Ceram Int.* **2011**, *37*, 393-398, DOI: 10.1016/j.ceramint.2010.08.017.

[45] Zhang, D. H.; Xue, Z. Y.; Wang, Q. P., Formation of ZnO nanoparticles by the reaction of zinc metal with aliphatic alcohols. *J. Phys. D* **2002**, *35*, 2837-2840, DOI: 10.1088/0022-3727/35/21/321.

[46] Harding, F. J., Breast cancer: Cause-prevention-cure. Tekline Publishing 2007, ISBN-13: 978-0955422102.

[47] Sunita, J.; Gaikwad, S.; Nimse, M.; Rajbhoj, A., Copper oxide nanoparticles: Synthesis, characterization and their antibacterial activity. *J. Cluster Sci.* **2011**, *22*, 121-29, DOI: 10.1007/s10876-011-0349-7.

[48] Miroslav, Č.; Padil, V. V. T., Green synthesis of copper oxide nanoparticles using gum karaya as a biotemplate and their antibacterial application. *Int. J. Nanomedicine* **2013**, *8*, 889-898, DOI: 10.2147/IJN.S40599.

[49] Antony, A.; Dharaneedharan, S.; Heo, M. S.; Mok, Y. S., Copper oxide nanomaterials: Synthesis, characterization and structure-specific antibacterial performance. *Chem. Engin. J.* **2015**, *262*, 179-188, DOI: 10.1016/j.cej.2014.09.083.

[50] Yanping, X.; He, Y.; Irwin, P. L.; Jin, T.; Shi, X., Antibacterial activity and mechanism of action of zinc oxide nanoparticles against campylobacter jejuni. *Appl. Environ. Microbiol.* **2011**, *77*, 2325-31, DOI: 10.1128/AEM.02149-10.

[51] Aydin, S. B.; Hanley, L., Antibacterial activity of dental composites containing zinc oxide nanoparticles. *J. Biomed. Mater. Res.-Part B Appl. Biomater.* **2010**, *94*, 22-31, DOI: 10.1002/jbm.b.31620.